Available online at www.sciencedirect.com

ScienceDirect

Journal of the European Ceramic Society 30 (2010) 459–463

www.elsevier.com/locate/jeurceramsoc

Optical properties of porous silicon coated with ultrathin gold film by RF-magnetron sputtering

Chanseok Hong, Hohyeong Kim, Sunghoon Park, Chongmu Lee *

Department of Materials Science and Engineering, Inha University, 253 Yonghyeondong, Incheon 402-751, South Korea

---

Abstract

Optical properties of porous silicon (PS) with ultrathin gold (Au) coatings were investigated. The gold films were deposited by using an RF-sputter-deposition technique on PS prepared by electrochemical anodization of P-type (1 0 0) Si. Photoluminescence (PL) spectroscopy and UV/VIS photospectroscopy analyses were performed to investigate the PL and optical transmittance properties of the Au-coated PS samples. Fourier transform infrared (FTIR) spectroscopy and X-ray photoelectron emission spectroscopy (XPS) analyses were also performed to investigate the origin of the PL enhancement by Au deposition. The PL intensity of PS is 6.4% increased by depositing 5.3 nm Au film using an RF-sputtering technique, but it is decreased 28.4% by postannealing. FTIR, spectrophotometry and XPS analysis results suggest that the PL enhancement by Au film deposition is attributed to the oxidation inhibiting effect of the Au film. However, it is not desirable to deposit an Au film thicker than 5.3 nm on PS as the PL intensity is decreased rather than increased owing to a significant decrease in the transmittance. Deterioration in the PL of the Au-coated PS by postannealing is ascribed to oxidation of the PS layer occurring at the high annealing temperature in spite of the Au passivation.

Keywords: Photoluminescence; Porous silicon; Gold; Transmittance; Annealing; X-ray photoelectron spectrometry

---

1. Introduction

During last two decades, a large amount of research work has been done to realize porous silicon (PS)-based optoelectronic devices such as light emitting diodes (LED),[1,2] waveguides,[3] optical filters,[1,2] photovoltaic diodes[4–8] and various types of sensors.[1] It is true that PS is a potent light emitting material showing significant luminescence over a wide range of spectrum. Optoelectronic devices based on PS have, however, not been commercialized yet because of the low luminescence efficiency due to a very low electrical conductivity and degradation of luminescence.[9]

To achieve photoluminescence (PL) with higher intensity and stability metal-passivated PS optoelectronic devices have also been proposed. Thin transparent conducting oxide films and ultrathin semi-transparent metal layers were used to improve the PL intensity in the hope that the conductivity and thus the PL of PS will be enhanced by filling the pores of PS with those materials with high conductivity. Those materials include indium tin oxide (ITO),[10–12] Al-doped ZnO(AZO),[13] Ga-doped ZnO(GZO),[14] Cu,[15] Ag,[16,17] and Au.[18,19] These passivation films have been deposited by various techniques including electroplating,[16] electrochemical anodization,[20] sputtering,[14] electron beam evaporation.[21]

In our previous report, we reported that the PL intensity of PS can be increased by 78% by depositing 9.2 nm Ag film on it. FTIR and XPS analysis revealed the PL enhancement by Ag film deposition is attributed to change in the bond structure from Si–H bonds to Si–Ag bonds and an increase in charge carrier concentration. In the present work, we report effect of Au film deposition by using RF-magnetron on the PL property of PS.

2. Experimental

PS samples for this study were formed by electrochemical etching (anodization) of 10–12 Ω cm P-type (1 0 0) silicon wafer at a current intensity of 50 mA/cm^2 using 1:1 solution of HF and ethanol in a Teflon container. The details of the anodization process and the anodization cell used for PS sample preparation are described in Ref. [13].

Ultrathin semi-transparent Au films were deposited by using radio frequency (RF) magnetron sputtering at room temperature on a part of the surface area (23 mm^2) of the PS layer. The RF

---

* Corresponding author. Tel.: +82 328607536; fax: +82 328625546.
E-mail address: cmlee@inha.ac.kr (C. Lee).

0955-2219/$ – see front matter © 2009 Elsevier Ltd. All rights reserved.
doi:10.1016/j.jeurceramsoc.2009.08.010

power and the chamber pressure, and the Ar gas flow rate in the sputtering process were 300 W, 0.05 Torr, and 30 sccm, respectively. The sputtering time was varied from 5 to 20 s with an increment of 5 s to obtain various film thicknesses. Au-coated PS samples were optionally annealed at 700 °C for 1 h in a vacuum annealing furnace. The base vacuum pressure in the furnace was 10^{-3} Torr.

PL spectroscopic analysis of the Au-deposited PS samples were performed at room temperature with the 325 nm line from a He–Cd laser (Kimon, 1K, Japan). The microstructures of the Au-coated PS samples were investigated using scanning electron microscopy (SEM: Hitachi S 4200). The thicknesses of the Au films deposited on the PS layers were determined from the reference plot of the Au films thickness vs. the sputtering time obtained for a fixed set of sputtering process parameters before the sputtering processes for the real sample preparation. Chemical bond structures at the Au–PS interfaces were investigated using Perkin-Elmer PHI-1600 X-ray photoelectron emission spectrometer (XPS) and a Nicolet 560 Fourier transform infrared (FTIR) spectrometer.

3. Results and discussion

Fig. 1(a) and (b) shows the PL spectra of as-deposited and annealed Au/PS samples, respectively. Both PL spectra have a rather broad peak ranging from 603 to 643 nm and the PL intensity at a wavelength of 643 nm is somewhat higher than that at a wavelength of 603 nm. The maximum PL intensities are plotted as functions of the Au layer thickness for both as-deposited and annealed samples in Fig. 2. The maximum PL intensity values of as-deposited and annealed samples with different Au film thicknesses read from Fig. 1(a) and (b) are also listed in Table 1. Fig. 2 and Table 1 tell us several interesting trends as follows: (1) the PL intensity of PS is increased by coating an ultrathin Au film as thin as 5.3 nm on it. (2) The PL intensity of PS decreases with continued increases in the Au film thickness from 5.3 nm. (3) The PL intensity of PS is decreased by thermal annealing. The PL enhancing effect of deposition of an ultrathin Au film on PS seems to be inferior to that of an ultrathin Ag film. According to our previous work[22] the maximum PL intensity was 77.7% increased from 224 to 398 by deposition

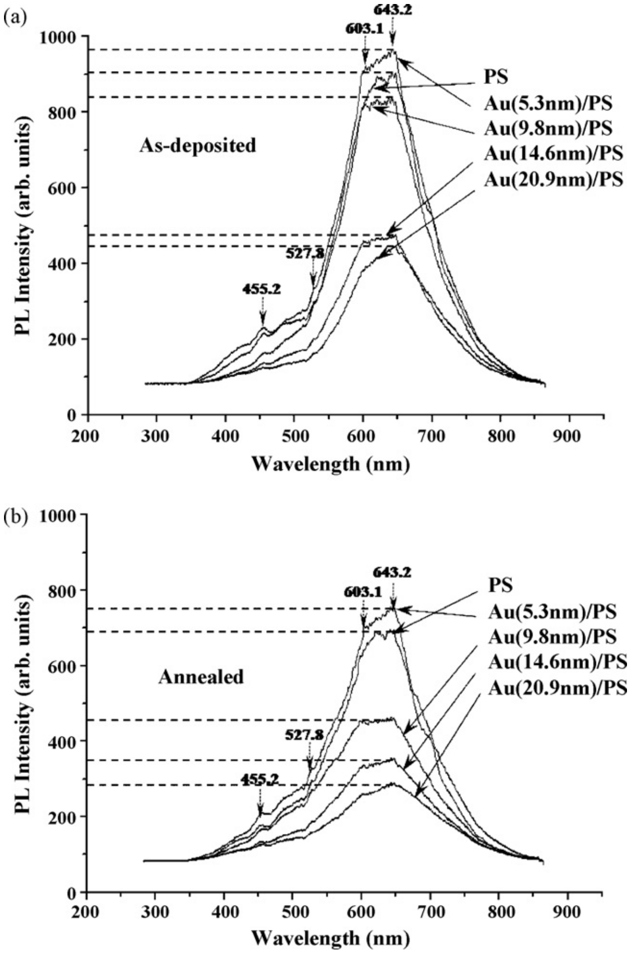

Fig. 1. The PL spectra of (a) as-deposited and (b) annealed Au/PS samples with different Au film thicknesses.

Table 1
The PL intensities and transmittances of as-deposited and annealed samples with different Au film thicknesses.

Sample	PL intensity at 643 nm	PL reduction percentage by annealing (%)	Sample	Transmittance at 643 nm (%)
PS				
As-deposited	895 ± 5	17.3	Bare glass	90 ± 1
Annealed	740 ± 5			
Au (5.3 nm)/PS				
As-deposited	952 ± 5	28.4	Au (5.3 nm)/glass	68 ± 1
Annealed	682 ± 5			
Au (9.8 nm)/PS				
As-deposited	813 ± 5	44.4	Au (9.8 nm)/glass	53 ± 1
Annealed	452 ± 5			
Au (14.6 nm)/PS				
As-deposited	464 ± 5	26.1	Au (14.6 nm)/glass	33 ± 1
Annealed	343 ± 5			
Au (20.9 nm)/PS				
As-deposited	420 ± 5	57.1	Au (20.9 nm)/glass	18 ± 1
Annealed	180 ± 5			

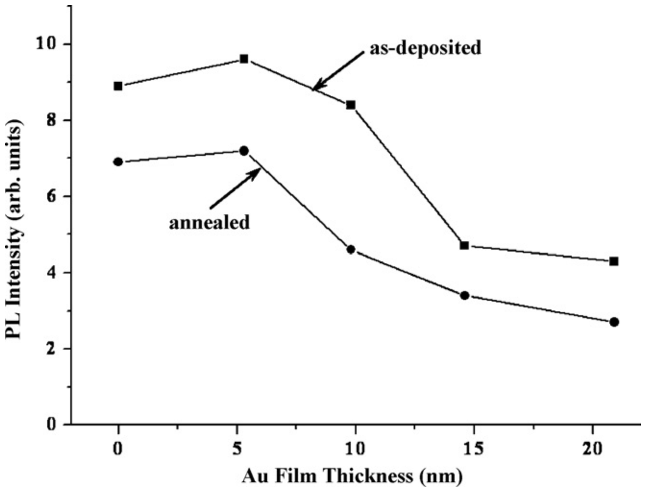

Fig. 2. The PL intensity of Au/PS samples at a wavelength of 570 nm as a function of Au film thickness.

of 9.2 nm Ag film. In contrast to it the present result shows that the maximum PL intensity has been 6.4 ± 1.2% increased from 895 ± 5 to 952 ± 5 by deposition of 5.3 ± 0.5 nm Au film. As regards the uncertainty of the PL measurement, the error limit of the measured PL intensity values is ±5. This error limit was determined through repeated measurements (for three times per sample) using the PL spectrometer used in this study. On the other hand, the error limit of the measured Au film thickness is surmised to be approximately ±0.5 nm. The thickness was determined from the reference plot of the Au films thickness vs. the sputtering time obtained for a fixed set of sputtering process parameters and an alpha step was previously used to measure film thicknesses for reference plotting. Therefore, the error limit of the film thickness may depend on the film thickness uniformity as well as the accuracy of the alpha step.

The inferiority of the Au film to the Ag film in the PL enhancing effect may be attributed to the lower electrical conductivity of Au than that of Ag. The electrical resistivity of Au and Ag are $0.452 \times 10^6\ \Omega^{-1}\ \text{cm}^{-1}$ [23] and $0.630 \times 10^6\ \Omega^{-1}\ \text{cm}^{-1}$ [23] respectively. According to previous reports[18] the PL and electroluminescence (EL) properties of PS can be enhanced by filling the pores of PS with a conductive material. Therefore, the inferior enhancement in the maximum PL intensity is ascribed to the lower electrical conductivity (or the higher electrical resistivity) of Au than that of Ag. The optical transmittance of a coating material can affect the PL property of the thin film coated on the PS before it reaches our eyes (Fig. 3). The optical transmittance of both the Au (5.3 nm)/glass sample and the Ag (9.2 nm)/glass sample is ∼68%, suggesting that there is almost no difference in transmittance between the two samples.

Fig. 4 shows the FTIR spectra of the as-deposited and annealed PS/Au samples. The two absorption bands centered around 870 and 2112 cm^{-1} are attributed to Si–H deformation vibration and stretching modes, respectively. The FTIR spectra clearly show that the intensities of the two absorption peaks located at wavelengths of about 870 and 2113 cm^{-1}, respectively, decrease by sputter-deposition of an Au film with a thickness of 9.8 nm on the PS layer and that both of the two peaks completely vanish by deposition of a 20.9 nm Au film. Disappearance of these two absorption bands associated with Si–H bonds by deposition of an ultrathin Au film on the PS layer is quite natural because the Si–H bonds are broken when the PS layer surfaces with Si–H termination are passivated with the Au films. The Si–H bonds seem to have been changed to more stable Si–Au bonds by Au passivation.

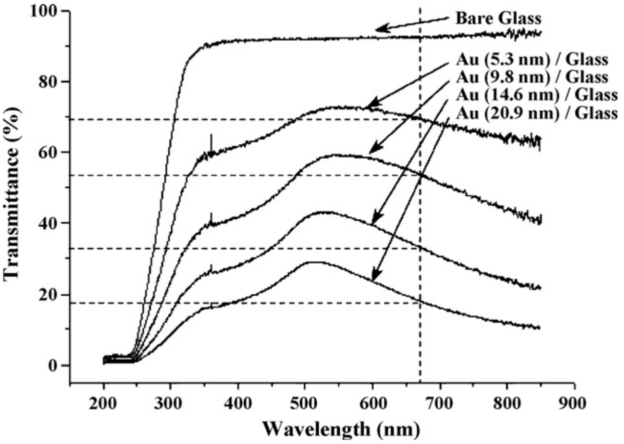

Fig. 3. The transmittance spectra of Au/glass samples with different Au film thicknesses.

On the other hand, the absorption peak of the broad absorption band in the wavelength range from 1033 to 1105 cm^{-1} associated with Si–O–Si bonds, has been decreased quite a bit by depositing a 9.8 nm Au film on the PS layer and has been decreased further by depositing a 20.9 nm Au film on the PS layers. This decrease in the absorption peak of PS by deposition of an Au film suggests that passivation of PS with the Au film can efficiently inhibit oxidation of PS surface. The PL intensity of PS at a wavelength of 643 nm strongly depends on the number of Si–O bonds at the PS surface and the optical transmittance of PS. The PL intensity tends to decrease as the number

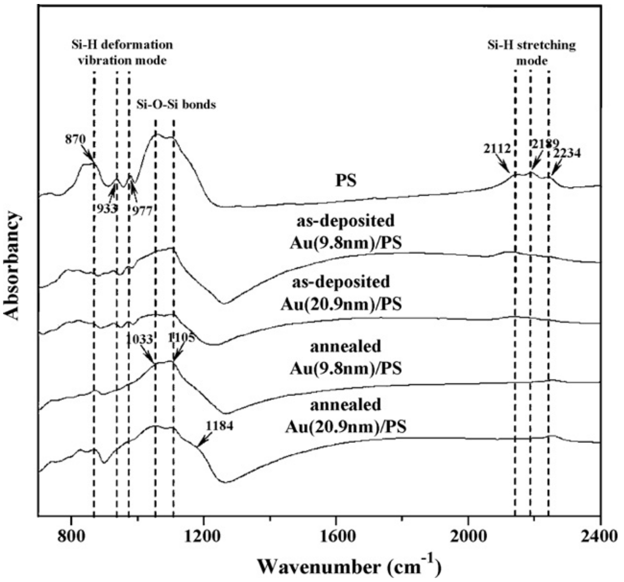

Fig. 4. The FTIR spectra of as-deposited and annealed Au/PS samples with different Au film thicknesses.

of Si–O bonds increases. On the other hand, the PL intensity tends to increase as the transmittance of PS increases. In comparison with the number of Si–O bonds in the Au (9.8 nm)/PS sample with that of the Au (20.9 nm)/PS sample, we can say that the former is larger than the latter, because the Si–O–Si bond peak of the Au (9.8 nm)/PS sample is higher than that of the Au (20.9 nm)/PS sample in Fig. 4. Yet, the transmittance of the Au (9.8 nm)/PS sample is higher than that of the Au (20.9 nm)/PS sample. We may extract a conclusion from the FTIR and transmittance data that transmittance makes a stronger effect on the PL intensity than the number of Si–O bonds since the PL intensity of the Au (9.8 nm)/PS sample is higher than that of the Au (20.9 nm)/PS sample. Also we may say that the PL enhancement by Au (9.8 nm) film deposition in spite of the transmittance deteriorating effect is attributed to the decrease in the number of Si–O bonds, in other words, oxidation inhibiting effect of the Au film.

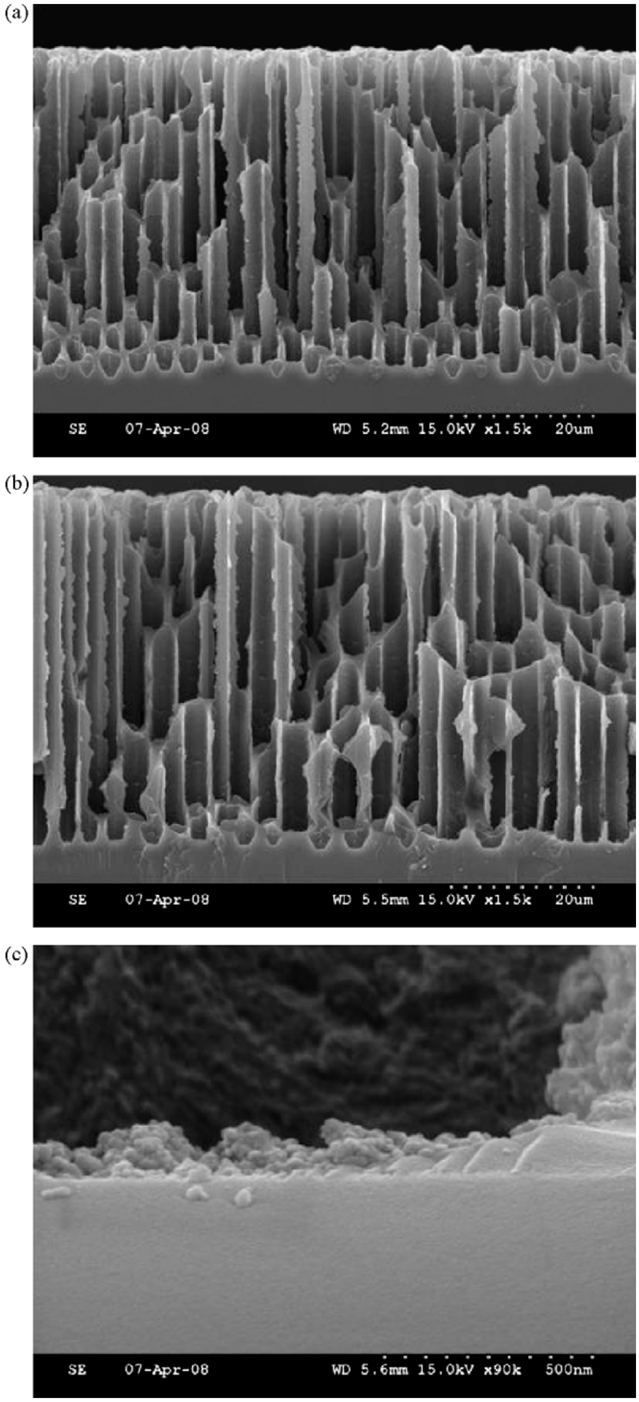

Fig. 5. Side view SEM images of (a) the PS sample and (b) the Au (20.9 nm)/PS sample and (c) a top view SEM image of the Au (20.9 nm)/PS sample.

In contrast to the as-deposited (or unannealed) samples high absorption peak of Si–O–Si bonds are found in the annealed samples. The growth of the Si–O–Si bond peak is ascribed to oxidation of the PS layers in spite of Au passivation. As can been seen from the SEM images of the Au-coated PS in Fig. 5(b) and (c), the ultrathin Au film cannot completely cover the PS surface with high porosity. Therefore, oxidation of the PS surface cannot be prevented effectively by Au passivation at the annealing temperature as high as 700 °C despite that Au is a strong oxidation-resistant material. Deterioration in the PL of the Au-coated PS by postannealing is ascribed to oxidation of the PS layer occurring at the high annealing temperature in spite of the Au passivation.

XPS Au 4f spectra of Au (9.8 nm)/PS and Au (20.9 nm)/PS samples are shown in Fig. 6. The Au (9.8 nm)/PS sample has two peaks located around 83 and 87 eV, while the Au (20.9 nm)/PS sample has two peaks located around 84 and 88 eV. According to Ref. [23], the photoelectron line peaks for Au°$4f_{7/2}$ and Au°$4f_{5/2}$ associated with Au–Au bonds located at 83.8 and 87.5 eV, respectively. Thus, the two peaks of each sample must be due to Au°$4f_{7/2}$ and Au°$4f_{5/2}$ associated with Au–Au bonds. The two kinds of peaks have shifted by ~1° toward the higher energy region as the Au film thickness increases from 9.8 to 20.9 nm. This shift is attributed to the increase in the number of Au–Au bond with an increase of the Au film thickness. Unlike the Au (20.9 nm)/PS sample there are high quantities of other Au bonds such as Au–Si bonds and Au–O bonds than Au–Au bonds in the Au (9.8 nm)/PS sample, which may have caused the two kinds of peaks to shift a little bit to the lower energy region.

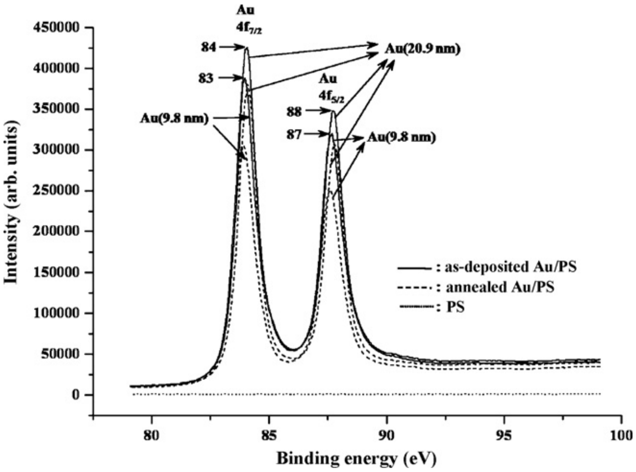

Fig. 6. XPS Au 4f spectra of as-deposited and annealed Au/PS samples along with a PS sample.

On the other hand, we cannot see any shift at all in the XPS peak position in the XPS spectra in Fig. 6 by thermal annealing, which implies that no other Au bonds such as Au–O bonds have formed during annealing. If a high quantity of Au–O bonds had formed during annealing the XPS Au $4f_{7/2}$ and Au $4f_{5/2}$ peaks associated with Au–Au bonds must have shifted.

4. Conclusions

Influence of deposition of semi-transparent Au ultrathin films on PS on the PL properties of the PS was investigated. The Pl intensity of PS is 6.4% increased by deposition of a 5.3 nm Au film using an RF-sputtering technique, but it is decreased 28.4% by postannealing at 700 °C for 1 h. FTIR, spectrophotometry, and XPS analysis results suggest that the PL enhancement by Au film deposition is attributed to the oxidation inhibiting effect of the Au film. Deterioration in the PL of the Au-coated PS by postannealing is ascribed to oxidation of the PS layer occurring at the high annealing temperature in spite of the Au passivation.

Acknowledgements

This work was supported by the Korea Science and Engineering Foundation (KOSEF) grant funded by the Korea government (MEST) (ROA-2007-000-20009-0).

References

1. Aliyu, Y. H., Morgan, D. V., Thomas, H. S. and Bland, W., AlGaInP LEDs using reactive thermally evaporated transparent conducting indium tin oxide (ITO). *Electron. Lett.*, 1995, **31**, 1691–1692.
2. Meng, L. J., Li, C. H. and Zhong, G. Z., The influence of the concentration of Er^{3+} ions on the characteristics of AC-electroluminescence in ZnS:ErF_3 thin films. *J. Lumin.*, 1987, **39**, 11–17.
3. Charrier, J., Guendouz, M., Haji, L. and Robert, P., Porosity gradient resulting from localised formation of porous Si: the effect on waveguiding. *Phys. Stat. Sol. (a)*, 2000, **182**, 431–436.
4. Tong, S., Liu, X. and Bao, X., Study of photoluminescence in nanocrystalline silicon/amorphous silicon multilayers. *Appl. Phys. Lett.*, 1995, **66**(4), 469–471.
5. Lyou, J., Yoon, K.-S., Kim, E. K. and Min, S.-K., Structural change and photo-response in porous poly-Si/Si. *Thin Solid Films*, 2000, **358**, 259–263.
6. Laiho, R. and Pavlov, A., Electronic properties and Schottky barrier of the porous silicon–Au interface. *Thin Solid Films*, 1995, **255**, 276–278.
7. Lazarouk, S., Bondarenko, V., La Monica, S., Maiello, G., Masini, G., Pershukevich, P. *et al.*, Electroluminescence from aluminum-porous silicon reverse-biased Schottky diodes formed on the base of highly doped n-type polysilicon. *Thin Solid Films*, 1996, **276**, 296–298.
8. Deresmes, D., Marissael, V., Stievenard, D. and Ortega, C., Electrical behaviour of aluminium-porous silicon junctions. *Thin Solid Films*, 1995, **255**, 258–261.
9. Jeske, M., Schultze, J. W., Thonissen, M. and Munder, H., Electrodeposition of metals into porous silicon. *Thin Solid Films*, 1995, **255**, 63–66.
10. Maruska, H. P., Namavar, F. and Kalkhoran, N. M., Current injection mechanism for porous-silicon transparent surface light-emitting diodes. *Appl. Phys. Lett.*, 1992, **61**, 1338–1340.
11. Futagi, T., Matsumoto, T., Katsuno, M., Ohta, Y., Mimura, H. and Kitamura, K., Visible electroluminescence from P-type crystalline silicon/porous silicon/N-type microcrystalline silicon carbon PN junction diodes. *Jpn. J. Appl. Phys.*, 1992, **31**, L616–L618.
12. Kozlowsk, F., Sauter, M., Steiner, P., Richter, A., Sandmaier, H. and Lang, W., Electroluminescent performance of porous silicon. *Thin Solid Films*, 1992, **222**, 196–199.
13. Kim, C., Park, A., Prabakar, K. and Lee, C., Physical and electronic properties of ZnO:Al/porous silicon. *Mater. Res. Bull.*, 2006, **41**, 253–259.
14. Prabakaran, R., Monteiro, T., Peres, M., Viana, A. S., Cunha, A. F. da, Aguas, H. *et al.*, Optical and structural analysis of porous silicon coated with GZO films using rf magnetron sputtering. *Thin Solid Films*, 2007, **515**, 8664–8669.
15. Ansari, Z. A., Hong, K. and Lee, C., Structural and electrical properties of porous silicon with rf-sputtered Cu films. *Mater. Sci. Eng. B*, 2002, **90**, 103–109.
16. Lu, X. W., Du, X. W., Sun, J., Han, X. and Kulinich, A., Influence of surface Si–Ag bonds on photoluminescence of porous silicon. *J. Appl. Phys.*, 2006, **100**, 063512.
17. Young, T. F., Liu, J. F., Wu, C. C., Fu, G. H. and Chen, C. S., Study of Ag thin films deposited on porous silicon. *Appl. Surf. Sci.*, 1996, **92**, 57–60.
18. Lang, W., Steiner, P. and Kozlowski, F., Porous silicon electroluminescent devices. *J. Lumin.*, 1993, **57**, 341–349.
19. Koshida, N. and Koyama, H., Visible electroluminescence from porous silicon. *Appl. Phys. Lett.*, 1992, **60**, 347–349.
20. Sun, J., Lu, Y. W., Du, X. W. and Kulinich, S. A., Improved visible photoluminescence from porous silicon with surface Si–Ag bonds. *Appl. Phys. Lett.*, 2005, **86**, 171905.
21. Tanaki, S., Matsumoto, K. and Suzuki, K., Properties of highly conducting ito films prepared by ion plating. *Appl. Surf. Sci.*, 1988, **33/34**, 919–925.
22. CHEMIX School Periodic Table with Electrical Conductivity Table: www.downloadtopc.Com.
23. Wagner, C. D., Riggs, W. W., Davis, L. E., Moulder, J. F. and Muilenberg, G. E., *Handbook of X-ray Photoelectron Spectroscopy*. Perkin-Elmer Corporation, Eden Prairie, Minnesota, USA, 1979, p. 185.